View metadata, citation and similar papers at core.ac.uk
brought to you by CORE
provided by Ulster University's Research Portal

Bioinformatics, YYYY, 0–0
doi: 10.1093/bioinformatics/xxxxx
Advance Access Publication Date: DD Month YYYY
Manuscript Category

Systems Biology

New models of atherosclerosis and multi-drug therapeutic interventions.

Andrew Parton[1#], Victoria McGilligan[1], Melody Chemaly[1], Maurice O'Kane[2] and Steven Watterson[1]*

[1]Northern Ireland Centre for Stratified Medicine, University of Ulster, Derry, Co Londonderry, Northern Ireland, United Kingdom

[2]Western Health and Social Care Trust, Altnagelvin Hospital, Derry, Co Londonderry, Northern Ireland, United Kingdom

*To whom correspondence should be addressed.

[#]Current Address: The European Bioinformatics Institute (EMBL-EBI), Wellcome Genome Campus, Hinxton, Cambridge United Kingdom

Associate Editor: XXXXXXX

Received on XXXXX; revised on XXXXX; accepted on XXXXX

Abstract

Motivation. Atherosclerosis is amongst the leading causes of death globally. However, it is challenging to study *in vivo* or *in vitro* and no detailed, openly-available computational models exist. Clinical studies hint that pharmaceutical therapy may be possible. Here we develop the first detailed, computational model of atherosclerosis and use it to develop multi-drug therapeutic hypotheses.

Results. We assembled a network describing atheroma development from the literature. Maps and mathematical models were produced using the Systems Biology Graphical Notation (SBGN) and Systems Biology Markup Language (SBML), respectively. The model was constrained against clinical and laboratory data. We identified five drugs that together potentially reverse advanced atheroma formation.

Availability and Implementation. The map is available in the supplementary information in SBGN-ML format. The model is available in the supplementary material and from BioModels, a repository of SBML models, containing CellDesigner markup.

Contact. s.watterson@ulster.ac.uk

Supplementary Information. Available from Bioinformatics online.

1 Introduction

Cardiovascular disease (CVD) is the primary cause of global mortality. CVD is estimated to account for 17.9m deaths worldwide each year, representing 31% of all-cause mortality worldwide (WHO, 2018) and 45% of all-cause mortality within Europe (Wilkins, 2017). Such a prevalent condition incurs a significant financial burden, accounting for 17% of all healthcare expenditure in the USA. Age is a significant risk factor and with an aging population, the cost of CVD related therapies is predicted to almost triple in the USA from $273 billion in 2010 to $818 billion by 2030 (Heidenreich, 2011).

Atherosclerosis is estimated to account for 71% of CVD diagnoses (Nichols, 2012). It is characterized by the hardening of an artery wall, and the formation of a fibrous-fatty lesion within the surface layer. As the disorder progresses, thick extracellular plaques of lipid build within

© The Author(s) (2018). Published by Oxford University Press. All rights reserved. For Permissions, please email: journals.permissions@oup.com

Downloaded from https://academic.oup.com/bioinformatics/advance-article-abstract/doi/10.1093/bioinformatics/bty980/5232220 by University of Ulster user on 20 December 2018

the artery wall, occluding the artery and reducing blood flow. Either as a result of plaque rupture or of the turbulent blood flow they induce, thrombosis can occur, further occluding the artery (Insull Jr, 2009; Parton, 2016).

Despite our increasing knowledge of the mechanisms involved in this disorder, its formation is still not fully understood. In part, this is due to the significant challenge inherent in studying live, dynamic plaques. Accessing plaques in vivo is logistically difficult, necessitating catheterization, and ethically challenging as it can increase the risk of plaque rupture. As a result, alternative approaches to studying the dynamics of atherosclerosis are needed. Computational modelling has the potential to be especially valuable here due to its flexibility, low financial and ethical cost, consistency and ease of replication. However, currently there are no computational or mathematical models of atherosclerosis that capture the molecular biology involved and are available to the research community for use in exploratory studies.

The molecular and cellular biology that mediates plaque formation can furnish drug targets for therapy development. Previous studies have typically focused on blood flow and plaque initiation (Parton, 2016; Di Tomaso, 2011; Silva, 2013) routinely omitting or simplifying details of the molecular and cellular biology for reasons of mathematical expediency (Bulelzai, 2012; Friedman, 2015; El Khatib, 2009). Critically, the resulting models have not been made publicly available with only one model pertaining to atheroma formation presently in the BioModels database (Chelliah, 2015), focusing on lipoprotein action and B-cell signaling with little detail on the mechanisms of plaque formation (Gomez-Cabrero, 2011). KEGG (Kanehisa, 2017), Reactome (Fabregat, 2016) and Wikipathways (Kutmon, 2011) contain no molecular biology maps of atherosclerosis. However models of contributory factors such as cholesterol metabolism do exist (Mazein, 2013; Watterson, 2013).

Here we develop the first detailed, predictive dynamical computational model of the formation of atherosclerosis using Systems Biology standards. The model is mapped using the Systems Biology Graphical Notation (SBGN) (Le Novere, 2009) and made available to the research community for reuse and refinement using the Systems Biology Graphical Notation Markup Language (SBGN-ML) (van Iersel, 2012). This map is accompanied by a mathematical model describing the dynamics of the interactions in the map as a system of ordinary differential equations (ODEs), made available using the Systems Biology Markup Language (SBML) (Hucka, 2003) and compatible with CellDesigner (Funahashi, 2008). There are many examples of SBGN and SBML compliant software (see http://sbgn.github.io/sbgn/software_support and http://sbml.org/SBML_Software_Guide respectively).

Currently, treatment of atherosclerosis focuses on limiting disease progression (though smoking cessation, lipid lowering, and anti-platelet therapies and optimal management of hypertension and diabetes) and revascularization procedures such as angioplasty and bypass grafting to clinically relevant stenotic lesions in the vasculature. Such treatments are clinically effective in managing patient risk. It is less clear whether therapies can reduce plaque size, although there is some evidence to suggest that intense statin treatment (Lima, 2004), combined statin-PCSK9 inhibitor treatment (Nicholls, 2016) or Cyclodextrin treatment (Zimmer, 2016) may yield a modest plaque reduction. New therapies that yield a substantial reduction in plaque size could have a dramatic impact on CVD morbidity and mortality and so their identification has high strategic importance. Here, we employ the model to develop effective therapeutic strategies comprising multi-drug combinations that reprogram disease dynamics leading to plaque regression.

2 Methods

A list of the cell types involved in atherosclerosis was compiled from the existing literature (see supplementary table S4). Each article identified was also searched for references to proteins and small molecules with each entity found considered for the model. A protein or small molecule was incorporated if its biological source, presence within a compartment and influence on atherogenesis (however minor) were all described. The model was assembled with CellDesigner (Funahashi, 2008) using SBGN with mass action and Michaelis-Menten equations primarily used to describe the dynamics. The resulting model was exported to SBGN-ML file format to disseminate the visual map and to SBML file format to disseminate the mathematical model. It was subsequently analysed using MATLAB software (https://www.mathworks.com).

We considered dynamics for three lipid profiles: high risk, medium-risk and low-risk comprising LDL concentrations of 190 mg/dl, 110 mg/dl (https://www.nhlbi.nih.gov/health/resources/heart/heart-cholesterol-hbc-what-html) and 50mg/dl (O'Keefe, 2004), respectively and HDL concentrations of 40 mg/dl, 50 mg/dl and 50 mg/dl, respectively (Boden, 2000). Atherosclerosis is considered to be a chronic condition. Hence, we considered plaque formation across a representative time scale of 80 years. The BRENDA enzyme database was searched for relevant known rate parameters (Placzek, 2017). In order to constrain parameters with unknown values, PubMed and Google Scholar searches were undertaken to find studies describing representative concentrations of the cells, proteins and small molecules involved. This enabled us to compile a series of clinical observations. Unknown parameters were optimized so as to maximize the agreement between the behavior of the model and these observations (see tables 1 and 2).

There are between 5 and 800 cells within a plaque area per high powered field (HPF) at 400x magnification (Brandl, 1997), where one HPF displays approximately 0.2mm2 of plaque area (Bonanno, 2000). We estimate that a plaque contains between 25 and 4000 cells per mm2. Average plaque area has been shown to be 15.2mm2 (von Birgelen, 1998), giving the number of cells in a plaque as being between 380 and 60800. Using this result and the references shown, we identified the quantitative and qualitative constraints outlined in tables 1 and 2.

The model was replicated in MATLAB and simulated using the non-stiff differential equation solver function 'ode23t'. To ensure accurate replication, the SBML version of the model was also simulated using the SBML ODE Solver built into CellDesigner. Initial conditions for each entity were estimated using control group data in cardiovascular disease studies (see supplementary table S3). Concentrations of LDL and HDL in the blood were kept constant, to reflect a stable patient context.

The resulting model contains 89 ordinary differential equations (ODEs), which are detailed in supplementary table S1.

2.1 Multi-drug plaque regression therapeutic hypotheses

To demonstrate the utility of the model, we undertook to identify an optimal multi-drug intervention hypothesis that would reprogram the dynamics of the model leading to regression of advanced plaques. It has been demonstrated that multidrug approaches have the potential to exploit compound effects to yield effective interventions at lower individual and collective dosages than in comparable single-drug interventions, reducing the risk from pleotropic effects (Benson, 2017). This is an example of the type of investigation that would be highly challenging to undertake in vivo yet can be undertaken computationally with ease.

Downloaded from https://academic.oup.com/bioinformatics/advance-article-abstract/doi/10.1093/bioinformatics/bty980/5232220 by University of Ulster user on 20 December 2018

We identified the following 9 drugs with targets in the model (targets in brackets): 2-(4-Chloro-3-(trifluoromethyl)phenoxy)-5-(((1-methyl-6-morpholino-2-oxo-1,2-dihydropyrimidin-4-yl)oxy)methyl)benzonitrile

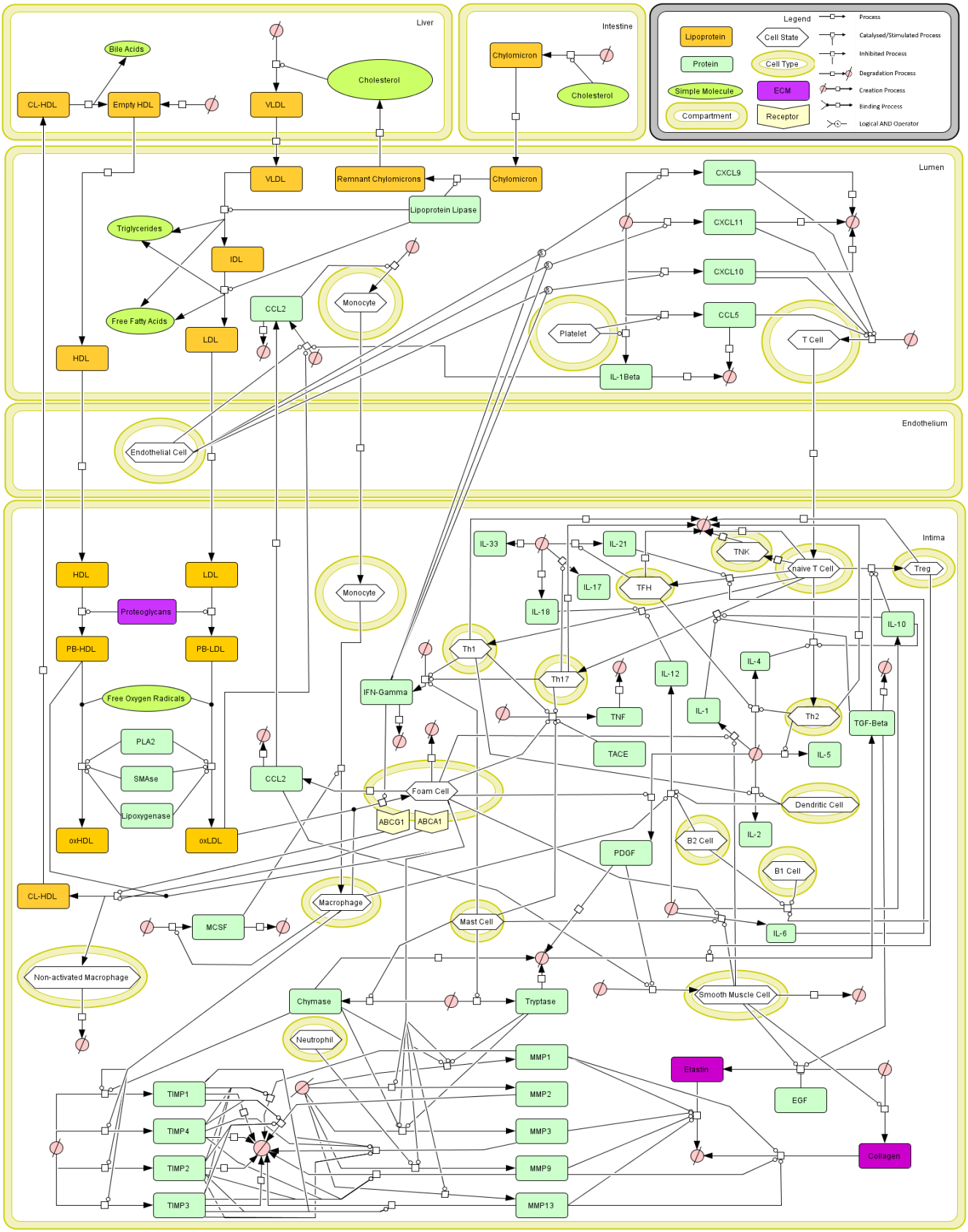

Figure 1. A map of atherosclerotic plaque dynamics shown using the Systems Biology Graphical Notation (SBGN).

Downloaded from https://academic.oup.com/bioinformatics/advance-article-abstract/doi/10.1093/bioinformatics/bty980/5232220 by University of Ulster user on 20 December 2018

(PLA2), GW4869 (SMase), Quercetin Monoglucoside (Lipoxygenase), cFMS Receptor Inhibitor III (MCSF), Bindarit (CCL2), Imatinib Mesylate (PDGF), Ustekinumab (IL12R), GSK1070806 (IL18R), SCH546738 (CXCL9, CXCL10, CXCL11, CCL5). Because PLA2, SMase and Lipoxygenase all catalyse the same interaction, we constrained these drugs to have the same concentration, giving a set of drugs with seven degrees of freedom.

We identified the optimal combination of drugs that would drive atherosclerosis regression using a genetic algorithm and a bespoke scoring function (see supplementary section S1) in MATLAB. A genetic algorithm was chosen for its ease of parallelisation and the transparency of its convergence. The analysis was run on an Intel(R) Xeon(R) CPU E5-2630 v3 @ 2.6GHz (Octo-core) CPU with 64GB of RAM running CentOS 7.

3 Results

A map of the model obtained is shown in Figure 1 using the SBGN schema. The model covers the liver, intestine, lumen, endothelium and tunica intima, including LDL retention, LDL oxidation, monocyte recruitment, monocyte differentiation, smooth muscle cell proliferation, phagocytosis, reverse cholesterol transport and T-cell proliferation. The cell types involved include monocytes, endothelial cells, T-cells, macrophages, foam cells, B-cells, smooth muscle cells, neutrophils, dendritic cells and mast cells. Each interaction represents a parameterized equation (see supplementary tables S1 and S2), enabling us to simulate the changing concentrations/abundances of the model as the plaque forms.

The initial conditions identified are described in supplementary table S3 and unknown parameters were optimized so that the model simultaneously satisfied the constraints described in tables 1 and 2. Along with figures S2, S3 and S4, tables 1 and 2 demonstrate consistency with the underlying unperturbed biology. Key markers for plaque development include smooth muscle cell, macrophage and foam cell and Th1 cell proliferation. Their behavior for the three risk profiles is shown in Figure 2.

3.1 Reusability of the model

The files can be opened, edited and analyzed in software supporting the SBGN-ML and SBML standards. SBML compliant software includes Copasi (Bergmann, 2017), Cytoscape with the cy3SBML plugin (König, 2012) and Dizzy (Ramsey, 2005). Supplementary Fig S1 shows the graphical map opened in three representative SBGN compliant editors: Newt (http://web.newteditor.org/), PathVisio (Kutmon, 2015) and VANTED with SBGN-ED extension (Czauderna, 2010) along with a subsection of the plain text, XML file.

3.2 Therapeutic hypothesis generation

We determined the following drug combination that optimally drove plaque regression. Concentrations are described as multiples of the corresponding inhibition constants, ki. 2-(4-Chloro-3-(trifluoromethyl)phenoxy)-5-(((1-methyl-6-morpholino-2-oxo-1,2-dihydropyrimidin-4-yl)oxy)methyl)benzonitrile (PLA2) – 4.35x10-5, GW4869 (SMase) – 4.35x10-5, Quercetin Monoglucoside (Lipoxygenase) – 4.35x10-5, Bindarit (CCL2) – 37.0, cFMS Receptor Inhibitor III (MCSF) – 0, SCH546738 (CXCL9, CXCL10, CXCL11, CCL5) – 8.45x10-4, Ustekinumab (IL12R) – 7.62, GSK1070806 (IL18R) – 7.60, Imatinib Mesylate (PDGF) – 0. As can be seen from Fig 3A, this combination was identified quickly with approximately optimal results being identified within 20 generations using a genetic algorithm. Figs 3B, 3C and 3D show the predicted dynamics of atherosclerosis after this intervention is applied at forty years following forty years of the high risk lipid profile. We can see that smooth muscle cells, macrophages and foam cells and Th1-cell counts are all rapidly driven down by the intervention.

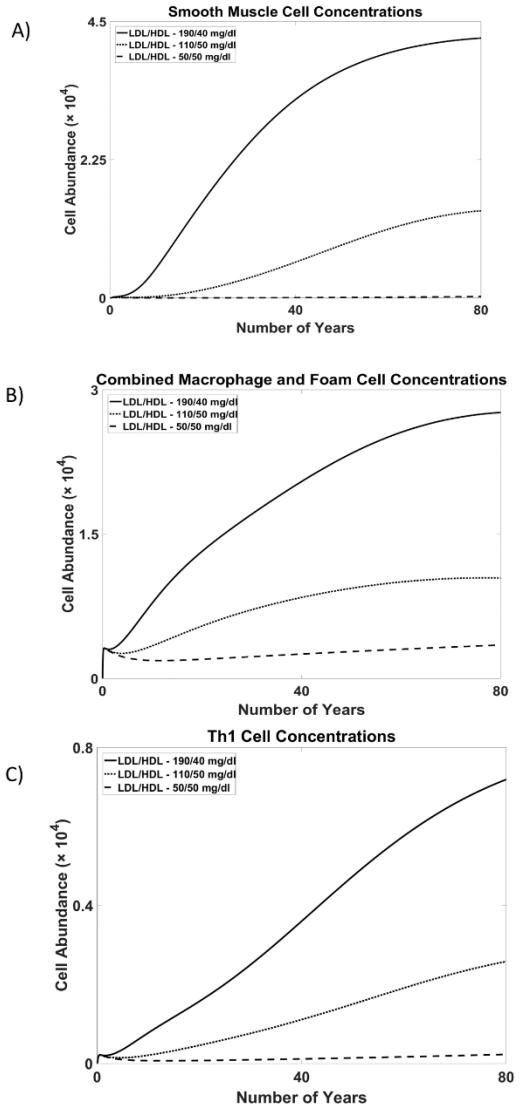

Figure 2. Key indicators of plaque formation during plaque development for the three blood LDL/HDL profiles: 190/40 mg/dl, 110/50 mg/dl and 50/50 mg/dl. (A) Smooth muscle cell concentrations. (B) macrophage and foam cell concentrations. (C) Th1 cell concentrations

4 Discussion

CVD is a large burden on healthcare worldwide. Front line therapies for the primary and secondary prevention of atherosclerotic disease include smoking cessation, lipid management, blood pressure control, optimal control of diabetes and the use of antiplatelet agents. However, the

Downloaded from https://academic.oup.com/bioinformatics/advance-article-abstract/doi/10.1093/bioinformatics/bty980/5232220 by University of Ulster user on 20 December 2018

number of pharmaceutical therapies is limited. By far the most commonly used
class of lipid lowering drugs is statins, which inhibit HMG-CoA reductase. Ezetimibe, a cholesterol absorption inhibitor, may be used in patients who are statin intolerant or who do not achieve lipid targets on the highest maximally targeted dose of statin. A new, recently licenced class of drugs, proprotein convertase subtilisin/kexin type 9 (PCSK9) inhibitors, suppress degradation of LDLR by PCSK9 and are associated with a significant reduction in serum LDL concentration and in cardiovascular events. Emerging drugs include Apolipoprotein B antisense drugs that suppress translation of ApoB, a key component of LDL, and microsomal triglyceride transfer protein inhibitors that induce significant LDL reduction (Henderson, 2016).

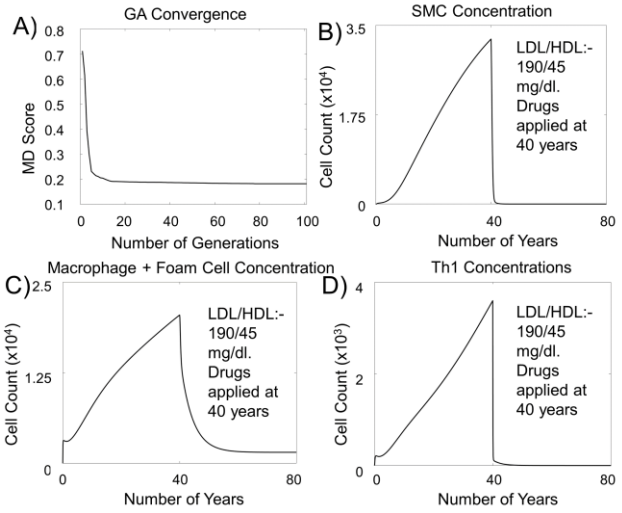

Figure 3. Therapeutic hypothesis generation. (A) Convergence on an atheroprotective multi-drug intervention hypothesis. (B – D) The impact of the identified intervention on key plaque constituents when applied after 40 years of plaque development at the high risk LDL/HDL profile of 190/40mg/dl.

Atherosclerotic plaques are highly challenging to study due to their location. In vivo study presents logistical and ethical challenges and there are few in vitro resources. Whilst they are not a replacement for in vivo studies, computational studies have the potential to contribute non-in vivo resources that can improve our understanding of CVD.

Here we have produced the first detailed, predictive model of atherosclerosis pathophysiology and it can serve as a resource for the research community to be reused, refined and expanded in future. Models of this type can be used to predict the on-target and off-target consequences of interventions. This can be exploited in single drug development to identify the drug targets that have the greatest potential therapeutic value or in multi-drug intervention development to identify drug combinations and target combinations with the greatest potential therapeutic value (Benson, 2017). The scale of the global CVD burden means that there is a pressing need to develop new pharmaceutical therapeutics that both address clinical need and can sustain the pharmaceutical industry as intellectual property protection expires around current therapeutics. Multi-drug interventions of the type identified here have a vast untapped potential to contribute to future therapeutics in this way.

The development of therapeutic hypotheses can form part of programmes of personalized or stratified medicine by adapting the parameters to individuals or to patient subgroups. Such parameterizations could be identified by optimizing the model to time course data or by determining the impact of single nucleotide polymorphisms on protein function.

The dynamics of the model show broad agreement with observed clinical results (see tables 1 and 2). Because the model describes spatial effects and cellular function very simply, it is unlikely to be able to recreate all clinical results exactly. Doing so would require greater complexity across length scales. However, we demonstrate order of magnitude agreement in almost all cases and show the correct qualitative dose responses. Optimizing the parameters so as to ensure a sufficiently large response to changes in lipoprotein profile for particular model components was challenging. Consequently, particular components are systematically over-estimated for the low LDL profile and the difference between high and low LDL profiles, although large, is not as great as that observed clinically. In changing the lipid profile, we adjusted the concentrations of LDL and HDL in the model. This logically does not impact upon components upstream of LDL and HDL. Hence, we would expect to see no resulting change in chylomicron or triglyceride concentrations as described in rows 28 and 29 of table 1. To see changes in chylomicron or triglyceride concentrations would require either modifying VLDL and IDL values across risk profiles or incorporating further feedback into the model.

Atherosclerosis is known to have comorbidities such as rheumatoid arthritis and depression (Gibson, 2017). By using incorporating ‘omic data from studies of other diseases, this model can be used to explore their impact on atherosclerosis as a comorbidity. Similarly, it can be used to explore the impact of therapies for other diseases on atherosclerosis either where there are targets in atherosclerosis associated pathways or through changes to ‘omic profiles.

The therapeutic hypotheses identified here could be validated and developed further by experimentation in animal models (Getz, 2012). Each animal model has limitations and none are a perfect surrogate for human atheroma. As a result, the computational model presented here would need to be adapted for each animal system and new therapeutic hypotheses would need to be generated. However, this would be the next step towards therapy development.

Funding

This work was supported by European Union Regional Development Fund (ERDF) EU Sustainable Competitiveness Programme for N. Ireland; the Northern Ireland Public Health Agency (Health and Social Care R&D); Ulster University [all to Professor Tony Bjourson]; and Microsoft Azure Research [CRM:0740357 to SW].

Conflict of Interest: The authors declare that they have no competing interests.

References

Adiguzel E, et al. (2009) Collagens in the progression and complications of atherosclerosis. *Vascular Medicine*. **14**(1), 73-89.

Arakelyan A, et al. (2005) Serum levels of the MCP-1 chemokine in patients with ischemic stroke and myocardial infarction. *Mediators of Inflammation* **2005**(3), 175–9.

Benson H, et al. (2017) Is systems pharmacology ready to impact upon therapy development? A study on the cholesterol biosynthesis pathway. *Br J Pharma* **174**(23), 4362-4382

Bergmann FT, et al. (2017) COPASI and its applications in biotechnology, J Biotechnol. **261**, 215-220.

Boden WE. (2000) High-density lipoprotein cholesterol as an independent risk factor in cardiovascular disease: assessing the data from Framingham to the

Downloaded from https://academic.oup.com/bioinformatics/advance-article-abstract/doi/10.1093/bioinformatics/bty980/5232220 by University of Ulster user on 20 December 2018

Veterans Affairs High-Density Lipoprotein Intervention Trial. *Am J Cardio* **86**(12), 19-22.
Bonanno E, et al. (2000). Flow cytometry analysis of atherosclerotic plaque cells from human carotids: A validation study. *Cytometry* **39**(2), 158–165.
Brandl R, et al. (1997). Topographic Analysis of Proliferative Activity in Carotid Endarterectomy Specimens by Immunocytochemical Detection of the Cell Cycle Related Antigen Ki-67. *Circulation* **96**(10), 3360–3368.
Bulelzai MA, et al. (2012) Long time evolution of atherosclerotic plaques. *J Theor Biol* **297**, 1–10.
Chelliah V, et al. (2015) BioModels: ten-year anniversary, *Nucl. Acids Res* **43**(D1), D542–D548
Czauderna T, et al. (2010) Editing, Validating, and Translating of SBGN Maps. *Bioinformatics* **26**(18), 2340-2341.
Delgado-Roche L, et al. (2015) Arresting progressive atherosclerosis by immunization with an anti-glycosaminoglycan monoclonal antibody in apolipoprotein E-deficient mice. *Free Radical Biol Med* **89**, 557-66.
Di Iorio A, et al. (2003). Serum IL-1b levels in health and disease: A population-based study. "The InCHIANTI study." *Cytokine* **22**(6), 198–205.
Di Tomaso G, et al. (2011) A multiscale model of atherosclerotic plaque formation at its early stage, *IEEE Trans Biomed Eng* **58**(12), 3460-63
El Khatib N, et al. (2009) Mathematical modelling of atherosclerosis as an inflammatory disease. *Phil Trans Roy Soc A: Math, Phys Eng Sci* **367**(1908), 4877-86.
Fabregat A, et al. (2016) The Reactome pathway Knowledgebase, *Nucl Acid Res* **44**(D1), D481-7.
Ferdousie VT, et al. (2017) Serum CXCL10 and CXCL12 chemokine levels are associated with the severity of coronary artery disease and coronary artery occlusion. *Int J Cardio* **233**, 23-8.
Ferns GA, et al. (1991) Inhibition of neointimal smooth muscle accumulation after angioplasty by an antibody to PDGF. *Science* **253**(5024), 1129-32.
Friedman A, et al. (2015) A Mathematical Model of Atherosclerosis with Reverse Cholesterol Transport and Associated Risk Factors, Bull Math Biol **77**(5), 758-781
Funahashi A, et al. (2008) CellDesigner 3.5: A Versatile Modeling Tool for Biochemical Networks, *Proc IEEE* **96**(8), 1254 – 1265.
Getz GS, Reardon CA (2012) Animal models of atherosclerosis. *Arterio, Thromb, Vasc Bio* **32**(5), 1104-15.
Gibson D, et al. (2017) Coincidence versus consequence: opportunities in multimorbidity research and inflammation as a pervasive feature, *Exp Rev Precis Med Drug Dev* **2**(3), 147-156
Gomez-Cabrero D, et al. (2011) Workflow for generating competing hypothesis from models with parameter uncertainty, *Interface Focus* **1**(3), 438-49.
Gonçalves I, et al. (2003). Changes related to age and cerebrovascular symptoms in the extracellular matrix of human carotid plaques. *Stroke* **34**(3), 616–22.
Grufman H, et al. (2004) Evidence for altered inflammatory and repair responses in symptomatic carotid plaques from elderly patients. *Atherosclerosis* **237**(1), 177-82.
Gupta S, et al. (1997) IFN-gamma potentiates atherosclerosis in ApoE knock-out mice, *J Clin Invest* **99**(11), 2752-61.
Hauer A, et al. (2005) Blockade of Interleukin-12 Function by Protein Vaccination Attenuates Atherosclerosis, *Circulation* **112**, 1054-1062.
Heidenreich PA, et al. (2011) Forecasting the future of cardiovascular disease in the United States: A policy statement from the American Heart Association. *Circulation*. **123**(8), 933-44.
Henderson R., et al. (2016) The genetics and screening of familial hypercholesterolaemia. *J Biomed Sci* **23**(1), 39.
Herder C, et al. (2011) RANTES/CCL5 and risk for coronary events: results from the MONICA/KORA Augsburg case-cohort, Athero-Express and CARDIoGRAM studies. *PLoS One* **6**(12), e25734
Herder C, et al. (2012) TGF-b1 content in atherosclerotic plaques, TGF-b1 serum concentrations and incident coronary events. *Euro J Clin Inv* **42**(3), 329–37.
Hoff H, et al. (1978). Apo B concentration in the normal human aorta. *Biochem Biophys Res Comm* **85**(4), 1424–1430.
Hucka M, et al. (2003) The systems biology markup language (SBML): a medium for representation and exchange of biochemical network models, *Bioinformatics* **19**(4), 524-31.
Insull Jr W. (2009) The pathology of atherosclerosis: plaque development and plaque responses to medical treatment. *Am J Med* **122**(1), S3-14.
Kanehisa M, et al. (2017) KEGG: new perspectives on genomes, pathways, diseases and drugs, *Nucl Acid Res* **45**(D1), D353-D361.
Kao J, et al. (2003). Elevated serum levels of the CXCR3 chemokine ITAC are associated with the development of transplant coronary artery disease. *Circulation* **107**(15), 1958–1961.
König M, et al. (2012) CySBML: a Cytoscape plugin for SBML, *Bioinformatics* **28**(18), 2402-3
Kutmon M, et al. (2015) PathVisio 3: An Extendable Pathway Analysis Toolbox, *PLoS Comp Bio* **11**(2), e1004085
Kutmon M, et al. (2016) WikiPathways: capturing the full diversity of pathway knowledge *Nucl Acid Res* **44**(D1), D488-D494.
Le Novere N, et al. (2009) The Systems Biology Graphical Notation. *Nat Biotech* **27**, 735–41.
Lima JA, et al. (2004) Statin-induced cholesterol lowering and plaque regression after 6 months of magnetic resonance imaging–monitored therapy, *Circulation* **110**(16), 2336-41.
Mazein A., et al. (2013) A comprehensive machine-readable view of the mammalian cholesterol biosynthesis pathway. *Biochem Pharma* **86**(1), 56-66.
Molloy KJ, et al. (2004). Comparison of levels of matrix metalloproteinases, tissue inhibitor of metalloproteinases, interleukins, and tissue necrosis factor in carotid endarterectomy specimens from patients on versus not on statins preoperatively. *Am J Cardio* **94**(1), 144–146.
Nichols M, et al. (2012) European Cardiovascular Disease Statistics 2012. European Heart Network, Brussels, European Society of Cardiology, Sophia Antipolis
Nicholls SJ, et al. (2016) Effect of Evolocumab on Progression of Coronary Disease in Statin-Treated Patients: The GLAGOV Randomized Clinical Trial. *JAMA* **316**(22), 2373-2384.
Nishi K, et al. (2002). Oxidized LDL in carotid plaques and plasma associates with plaque instability. *Arterio, Thromb, Vasc Biol* **22**(10), 1649–1654.
O'Keefe JH, et al. (2004) Optimal low-density lipoprotein is 50 to 70 mg/dl: lower is better and physiologically normal. *JACC* **43**(11), 2142-6.
Parton A, et al. (2016) Computational modelling of atherosclerosis. *Brief Bioinf* **17**(4), 562-575.
Placzek S, et al. (2017), BRENDA in 2017: new perspectives and new tools in BRENDA, *Nucl Acid Res* **45**(D1), D380–D388.
Qiao JH, et al. (1997) Role of Macrophage Colony-Stimulating Factor in Atherosclerosis: Studies of Osteopetrotic Mice. *Am J Pathol* **150**(5), 1687–1699.
Ragino YI, et al. (2012). Activity of the inflammatory process in different types of unstable atherosclerotic plaques. *Bull Exp Biol Med* **153**(2), 186–189.
Ramalho LS, et al. (2013). Role of mast cell chymase and tryptase in the progression of atherosclerosis: Study in 44 autopsied cases. *Ann Diag Path* **17**(1), 28-31.
Ramsey S, et al. (2005) Dizzy: stochastic simulation of large-scale genetic regulatory networks. *J Bioinform Comp Bio* **3**(2), 415-36.
Sakai N, et al. (2003). Measurement of fasting serum apoB-48 levels in normolipidemic and hyperlipidemic subjects by ELISA. *J Lipid Res* **44**(6), 1256–1262.
Silva T, et al. (2013). Mathematical modeling of atherosclerotic plaque formation coupled with a non-newtonian model of blood flow. In Conference Papers in Science 2013 (Vol. 2013). Hindawi.
Stein A., et al. (2008). Circulating endothelial progenitor cells decrease in patients after endarterectomy. *J Vasc Surg* **48**(5), 1217–1222.
Szodoray P, et al. (2006) TH1/TH2 imbalance, measured by circulating and intracytoplasmic inflammatory cytokines–immunological alterations in acute coronary syndrome and stable coronary artery disease. *Scandi J Immun* **64**(3), 336-344.
Trogan E, et al. (2006) Gene expression changes in foam cells and the role of chemokine receptor CCR7 during atherosclerosis regression in ApoE-deficient mice. *PNAS* **103**(10), 3781-6.
van Dijk RA, et al. (2015) A change in inflammatory footprint precedes plaque instability: a systematic evaluation of cellular aspects of the adaptive immune response in human atherosclerosis. *JAMA* **4**(4), e001403.
van Iersel MP, et al. (2012) Software support for SBGN maps: SBGN-ML and LibSBGN, *Bioinformatics* **28**(15), 2016-21.
von Birgelen C, et al. (1998) Atherosclerotic coronary lesions with inadequate compensatory enlargement have smaller plaque and vessel volumes: observations with three dimensional intravascular ultrasound in vivo. *Heart* **79**(2), 137-42.
Vickers K, et al. (2009) Relationship of lipoprotein-associated phospholipase A2 and oxidized low density lipoprotein in carotid atherosclerosis, *J Lipid Res* **50**(9), 1735-1743.
Watterson S, et al. (2013) A model of flux regulation in the cholesterol biosynthesis pathway: immune mediated graduated flux reduction versus statin-like led stepped flux reduction. *Biochimie* **95**(3), 613-621.
Westerterp M, et al. (2013) Deficiency of ATP-Binding Cassette Transporters A1 and G1 in Macrophages Increases Inflammation and Accelerates Atherosclerosis in Mice. *Circulation Research* **112**, 1456–1465 .
Whitman SC, et al. (2002) Interleukin-18 enhances atherosclerosis in apolipoprotein E−/− mice through release of interferon-γ. *Circulation Res* **90**(2), e34-8.

Downloaded from https://academic.oup.com/bioinformatics/advance-article-abstract/doi/10.1093/bioinformatics/bty980/5232220 by University of Ulster user on 20 December 2018

WHO (2018) Noncommunicable diseases country profiles 2018, World Health Organisation

Wilkins E, et al. (2017) European Cardiovascular Disease Statistics 2017 edition, European Heart Network.

Yu HT, et al. (2015). Serum monokine induced by gamma interferon as a novel biomarker for coronary artery calcification in humans. *Coronary Artery Disease* **26**(4), 317–321.

Zimmer S, et al. (2016), Cyclodextrin promotes atherosclerosis regression via macrophage reprogramming, *Sci Trans Med* **8**(333), 333ra50.

Downloaded from https://academic.oup.com/bioinformatics/advance-article-abstract/doi/10.1093/bioinformatics/bty980/5232220 by University of Ulster user on 20 December 2018

Quantitative Comparison				From literature				From model			
No	Measureable	Location	Units	Estimate source	Lower estimate	Upper estimate	Sole estimate	Lower prediction	Upper prediction	Sole prediction	Figure
1	Smooth muscle cell count	Plaque	cells	35.10% of cellular composition (Bonanno, 2000)	133	21341		230	42287		2A
2	Macrophage (including foam cell) count	Plaque	cells	34.07% of cellular composition (Bonanno, 2000)	129	20715		3463	27630		2B
3	Th1 cell count	Plaque	cells	Ratio of Th1 to non-Th1 cells approximately 0.3 (van Dijk, 2015)	88	14031		223	7186		2C
4	MCP1/CCL2 concentration	Blood serum	pg/ml	myocardial infarction and ischemic stroke patients (Arakelyan, 2005)	100	775		163.8	649.8		S2.1
5	CXCL9 concentration	Blood serum	pg/ml	patients assessed for coronary artery calcium deposits (Yu, 2015)	17.4	271.2		23.8	283.9		S2.2
6	CXCL10 concentration	Blood serum	pg/ml	patients assessed for coronary artery disease (Ferdousie, 2017)	127.6	956.5		120.9	850.0		S2.3
7	CXCL11 concentration	Blood serum	pg/ml	control groups in transplantation studies (Kao, 2003)	420	1062		355	965		S2.4
8	IL1b concentration	Blood serum	pg/ml	congestive heart failure and control patients (Di Iorio, 2003)	0.28	2.12		0.97	2.04		S2.5
9	TIMP1 concentration	Plaque	µg/g	carotid endarterectomy patients, per wet weight plaque (Molloy, 2004)	5.3	12.4		3.6	11.5		S2.6
10	IFNg concentration	Plaque	pg/g	carotid endarterectomy patients, per wet weight plaque (Grufman, 2004)	20	182		5	167		S2.7
11	TGFb concentration	Plaque	mg/g	control and coronary artery disease patients, per weight protein (Herder, 2012)	0.33	0.76		0.05	0.80		S2.8
12	Chymase to tryptase density ratio	Plaque	none	(Ramalho, 2013)			107.8:135.1			106.0:134.3 high risk profile.	S2.9
13	T cell count	Plaque	cells	30.82% of cellular composition (Bonanno, 2000)	117	18739		8012	18562		S2.10
14	CCL5 concentration	Blood serum	ng/ml	control and coronary event patients (Herder, 2011)	2.7	176.0		45.7	181.1		S2.11
15	MMP1 concentration	Plaque	ng/g	carotid endarterectomy patients, per wet weight plaque (Molloy, 2004)	18	104		0.2	86.8		S2.12
16	MMP9 concentration	Plaque	ng/g	carotid endarterectomy patients, per wet weight plaque (Molloy, 2004)	121	722		1.6	609.6		S2.13
17	IL1b concentration	Plaque	ng/g	carotid endarterectomy patients, per wet weight plaque (Molloy, 2004)	12	24		0.1	23.6		S2.14
18	IL6 concentration	Plaque	µg/g	carotid endarterectomy patients, per wet weight plaque (Molloy, 2004)	1.5	5.1		0.025	5.3		S2.15

Downloaded from https://academic.oup.com/bioinformatics/advance-article-abstract/doi/10.1093/bioinformatics/bty980/5232220 by University of Ulster user on 20 December 20

19	TNFa concentration	Plaque	ng/g	carotid endarterectomy patients, per wet weight plaque (Molloy, 2004)	15	27		0.3	24		S3.1
20	IL10 concentration	Plaque	ng/g	arterial occlusion patients, ranging per wet weight plaque (Stein, 2008)	1.51	2.29		0.6	2.1		S3.2
21	IL12 concentration	Plaque	ng/g	arterial occlusion patients, per wet weight plaque (Stein, 2008)	3.6	4.6		0.7	5.2		S3.3
22	Elastin concentration	Plaque	mg/g	acute coronary syndrome patients, per wet weight plaque (Gonçalves, 2003)			1.58			1.85 high risk profile	S3.4
23	Collagen concentration	Plaque	mg/g	acute coronary syndrome patients, per wet weight plaque (Gonçalves, 2003)			6.26			4.87 high risk profile.	S3.5
24	PDGF concentration	Plaque	pg/g	carotid endarterectomy patients, per wet weight plaque (Grufman, 2004)	279	1381		2	1048		S3.6
25	Oxidized LDL concentration	Plaque	µg/g	weight of oxidized LDL per weight ApoB is 19.6 ng/µg in plaques and 1.9 ng/µg in normal intimal tissue (Nishi, 2002). Plaque concentration of ApoB ranges from 1.97 µg/mg to 0.13 µg/mg (Hoff, 1978)	0.25	38.6		2.6	36.8		S3.7
26	IL2 concentration	Plaque	ng/g	acute coronary syndrome patients, per weight protein (Ragino, 2012)			24.0			27 high risk profile	S3.8
27	IL18 concentration	Plaque	ng/g	acute coronary syndrome patients, per weight protein (Ragino, 2012)			10.7			10.9 high risk profile	S3.9
28	Chylomicron concentration	Blood serum	µg/ml	control and hyperlipidemic patients (Sakai, 2003)	1.4	52.6		49.1l	49.1		S3.10
29	Triglyceride concentration	Blood serum	mg/dl	control and hyperlipidemic patients (Sakai, 2003)	58	1005		754	754l		S3.11

Table 1: Quantitative constraints applied to the model.

Downloaded from https://academic.oup.com/bioinformatics/advance-article-abstract/doi/10.1093/bioinformatics/bty980/5232220 by University of Ulster user on 20 December 20

Qualitative comparison		From literature		From model	
No	Measureable	Location	Estimate source	Predicted behaviour	Figure
30	Atherogenic cell count	Plaque	Ratio of Th1 to Th2 cell count correlates with atherogenesis (Szodoray, 2006)	For high risk profile, increasing rate parameter of differentiation to Th1 cells by 10% and decreasing rate parameter of differentiation to Th2 cells by 10% increases foam cell counts.	S3.12
31	Atherogenic cell counts	Plaque	Animal models show plaque reduction mediated by reverse cholesterol transport after reducing lipid profile (Trogan, 2006)	Oxidized LDL concentration, smooth muscle cell count and foam cell count reduce when high risk profile switched to low risk profile.	S3.13, S3.14, S3.15
32	Atherogenic cell counts	Plaque	Blocking endogenous IL-12 has been shown to reduce atherogenesis (Hauer, 2005)	Reducing the rate parameter for IL-12 production by 75%, reduces foam cell count.	S4.1
33	Atherogenic cell counts	Plaque	Deficiency of ABCA1 function impairs reverse cholesterol transport, increases atheroma size (Westerterp, 2013)	Reducing the initial ABCA1 concentration by 90%, increases foam cell concentration.	S4.2
34	Macrophage and monocyte cell count	Plaque	Deficiency of MCSF reduces monocyte/macrophage circulation, plaque formation (Qiao, 1997)	Reducing the initial MCSF concentrations from 100 mg/g of tissue to 0 reduces macrophage count.	S4.3
35	T cell count	Plaque	IFNGR knockout reduces T-cells abundance (Gupta, 1997)	Decreasing the rate parameter for IFNG production by 50% reduces T-cell abundance.	S4.4
36	Atherogenic cell count	Plaque	IL-18 increases are atherogenic (Whitman, 2002)	Increasing the rate parameter for IL-18 production by 50%, increases smooth muscle cell recruitment.	S4.5
37	Oxidized LDL concentration	Plaque	Reducing proteoglycan concentration reduces intimal oxLDL concentrations (Delgado-Roche, 2015)	Decreasing the initial concentration of proteoglycan concentration from 500 to 100 mg/g of tissue reduces oxidized LDL concentration.	S4.6
38	Collagen concentration	Plaque	Increasing matrix metalloproteinase activity leads to degraded extracellular matrix (Adiguzel, 2009)	Doubling the rate parameter for binding between extra cellular matrix and matrix metalloproteinases reduces collagen concentrations.	S4.7
39	Atherogenic cell count	Plaque	PLA2 concentration correlates with atherogenesis (Vickers, 2009)	Reducing initial PLA2 concentration by 90% reduces foam cell count.	S4.8
40	Smooth muscle cell count	Plaque	Increasing PDGF activity increases smooth muscle cell abundance (Ferns, 1991)	Increasing the rate parameter for PGDF production by 200% increases smooth muscle cell recruitment.	S4.9

Table 2: Qualitative constraints applied to the model.

Downloaded from https://academic.oup.com/bioinformatics/advance-article-abstract/doi/10.1093/bioinformatics/bty980/5232220 by University of Ulster user on 20 December 2018